Cathodoluminescence study on dislocations in silicon

T. Sekiguchi[a] and K. Sumino[b]
Institute for Materials Research, Tohoku University, Sendai 980-77, Japan

(Received 18 September 1995; accepted for publication 1 December 1995)

A study was made on the characteristics of cathodoluminescence (CL) from Si crystals with various configurations of dislocations. D3 and D4 were observed along slip lines, while D1 and D2 were found to be strong in the region where plural slip lines intersect each other. It was shown that not only Lomer–Cottrell dislocations but also jogs act as recombination centers for D1 and D2 luminescence. The spatial distributions of D1 and D2 luminescence were observed to be similar to each other, this was also true of D3 and D4. The effect of hydrogenation on CL distribution was also investigated. Contrary to the reports of other groups, no evidence was obtained on the enhancement of D line luminescence due to metal contamination. © *1996 American Institute of Physics.* [S0021-8979(96)08705-1]

I. INTRODUCTION

It is well known that plastic deformation introduces a high density of deep energy levels into silicon crystals. The study of thermal stability has confirmed that these deep levels detected by electrical measurements originate from defects other than dislocations, since they disappear during high temperature annealing while dislocations still remain.[1–3] Recent theoretical study also supports this idea showing that dislocations are accompanied by no deep levels,[4,5] but only by shallow levels originating from the deformation potential.[6,7]

On the other hand, dislocations in silicon crystals show characteristic luminescence, first observed by Dorozdov *et al.*[8,9] It is composed of 4 lines denoted by D1, D2, D3, and D4 whose peaks are located at 0.812, 0.875, 0.934, and 1.000 eV, respectively. This suggests that dislocations accompany some deep levels which act as radiative recombination centers. It is worth while to clarify the nature of dislocation-related luminescence.

Various characteristics of this luminescence have been studied so far, for example, dependence of luminescence intensity on the observation temperature,[10] the dependence of spectrum on the dominant type of dislocations,[11,12] thermal stability of the defect giving rise to luminescence,[13] effect of uniaxial stress on the peak energy,[14,15] polarization,[16,17] and so on.

Suezawa and Sumino[10,13,14,16] confirmed in a high temperature annealing experiment that dislocations themselves are active as recombination centers. They concluded that dangling bonds at the dislocation core are not responsible for the recombination processes but rather that reconstructed bonds or severe distortion at the dislocation core contribute to the radiative recombination processes. They also suggested that D1 and D2 lines originate from geometrical kinks at dislocations.

Sauer *et al.*[11] introduced rather straight dislocations lying parallel to the ⟨110⟩ directions by deformation at a low temperature under high stress. They discovered D12, D5, and D6 lines besides D1–D4. They studied the thermal stability of these lines and the dependence of their energy positions on the uniaxial stress. They concluded that the defects giving rise to the D3, D4, D5, and D6 lines are closely related to each other, whereas those giving rise to the D1 and D2 lines might be deformation-produced point defects in the vicinity of dislocations. They later concluded that the D3, D4, and D5 lines originate from the radiative recombination at the dissociated glide dislocations.[15]

There have been a few studies on the correlation of the photoluminescence (PL) spectrum with dislocation configuration or type of dislocation. Weronek *et al.*[17] introduced glide dislocations of a single slip system into float-zone grown Si crystals and observed the orientation dependence of the intensity and polarization of the D lines. The D1 and D2 lines showed a pronounced linear polarization with the electric vector of $E//[\bar{1}11]$ if detected from the [011] and $[2\bar{1}1]$ propagation direction of the light. They proposed that the D1 and D2 lines originate from the intrinsic stacking fault bounded by Shockley partial dislocations. The D3 and D4 lines showed rather complex polarization behavior. They were not successful in correlating the polarization with the geometry of dislocations. They also concluded that D3 was a TO phonon replica of D4 and that D1 was an O^{Γ} phonon replica of D2.

Lelikov *et al.*[12] observed PL spectra from various Si crystals containing various types of dislocations and stacking faults. They related the magnitude of the edge component of the Burgers vector of a dislocation with the peak energy of a D line. They concluded that the D1 line originates from Lomer–Cottrell dislocations, D2 from Frank partials, and D3 and D4 both from 90° partial dislocations.

Since we cannot introduce any given type of defects dominantly by plastic deformation, it is difficult to correlate the type of dislocation with the peak of the spectrum by means of conventional photoluminescence. Spatially resolved study such as cathodoluminescence (CL) is required to study the correlation between the type of dislocation and a luminescence line. Higgs *et al.*[18] obtained CL images of slip lines in a plastically deformed specimen and found that the D3 and D4 lines were strong along slip lines, whereas the D1 and D2 lines were predominant in the regions between the

[a]Electronic mail: sekiguch@dp.imr.tohoku.ac.jp
[b]Present address: Nippon Steel Corp., Futtsu-shi 293, Japan.

TABLE I. Primary slip systems and the possible dislocation reaction.

Compression axis	[123]	[110]	[120]	[11 11 $\bar{6}$]
Primary slip system	$\frac{a}{2}[101](\overline{111})$	$\frac{a}{2}[101](\overline{111})$ $\frac{a}{2}[011](\overline{111})$ $\frac{a}{2}[01\bar{1}](111)$ $\frac{a}{2}[\bar{1}01](111)$	$\frac{a}{2}[101](\overline{111})$ $\frac{a}{2}[\bar{1}01](111)$	$\frac{a}{2}[101](\overline{111})$ $\frac{a}{2}[011](\overline{111})$
Schmid factor	0.466	0.408	0.490	0.399
most probable reaction		$\frac{a}{2}[101](\overline{111})$ $+\frac{a}{2}[01\bar{1}](111)$ Lomer–Cottrell $\frac{a}{2}[101](\overline{111})$ $+\frac{a}{2}[\bar{1}01](111)$ jog–jog formation	$\frac{a}{2}[101](\overline{111})$ $+\frac{a}{2}[\bar{1}01](111)$ jog–jog formation	no reaction (repel)

slip lines. They attributed the D1 and D2 lines to impurities incorporated at the dislocation core. Their conclusion was different from those of previous works. We introduced dislocations with various configurations into silicon crystals avoiding metallic contamination, observed their CL images, and correlated each D line with the type of defect.

II. EXPERIMENT

Specimens used in this study were cut from a P-doped Si crystal grown by the float-zone (FZ) method whose resistivity was 0.4 Ω cm. Parallelepiped specimens $3\times4\times14$ mm^3 in size were cut along compression axes and finished by chemical polishing with HF:5HNO_3. Dislocations were introduced into specimens by compressive deformation. The compression axes were chosen parallel to the [123], [110], [120], and [11 11 $\bar{6}$] directions to realize different kinds of dislocation configurations. In the latter three conditions, the Schmid factors of other slip systems were smaller than one half that of primary slip systems. The possible reactions of dislocations belonging to the primary slip systems are listed in Table I.

Specimens were compressed with a resolved shear stress of 15 MPa for 5 min at 800 °C followed by cooling to room temperature under a stress of 7.5 MPa. The stress during cooling was applied to keep the dislocation lines straight. Inhomogeneous distribution of dislocation was realized by deformation under the above conditions. The configurations of both slip planes and slip lines of primary slip systems are given in Fig. 1. The bold lines show the dislocation loops generated from the front surface. The bold arrows show the directions of Burgers vectors.

Specimens, which were rinsed with RCA solution ($HCl:H_2O_2:H_2O=1:1:5$ and then $NH_4OH:H_2O_2:H_2O=1:1:5$),[19] were separated from a compression jig made of Mo by 2-mm-thick quartz plates. Heating was conducted by an infrared image furnace installed outside a deformation chamber made of high purity quartz. Deformation was done in an ambient of flowing Ar gas. These procedures were effective for avoiding contamination by metallic impurities.

Surface regions of deformed specimens were removed to a depth of about 50 μm by chemical etching prior to the CL

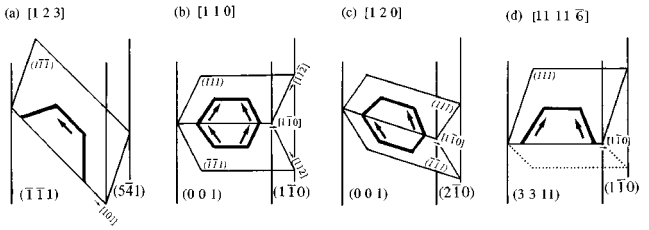

FIG. 1. Geometry of primary slip planes in (a) the [123]-, (b) [110]-, (c) [120]-, and (d) [11 11 6]-compressed specimens. The broad lines and arrows show the dislocation lines and the Burgers vectors, respectively, belonging to the primary slip systems.

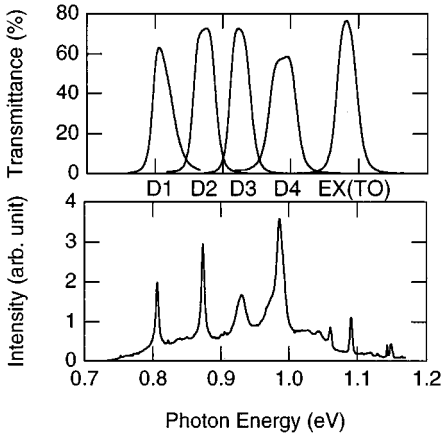

FIG. 2. Characteristics of band-pass filters and an example of a photoluminescence spectrum obtained from a lightly deformed specimen.

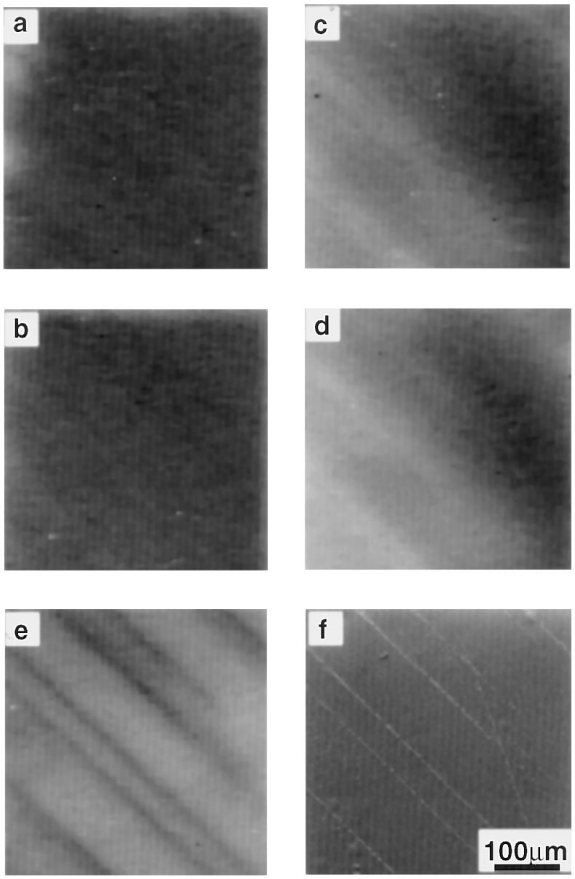

FIG. 3. A set of CL filtered images of the $(\overline{111})$ surface of the [123] compressed specimen: (a) D1, (b) D2, (c) D3, (d) D4, (e) EX(TO) images, and (f) secondary electron image.

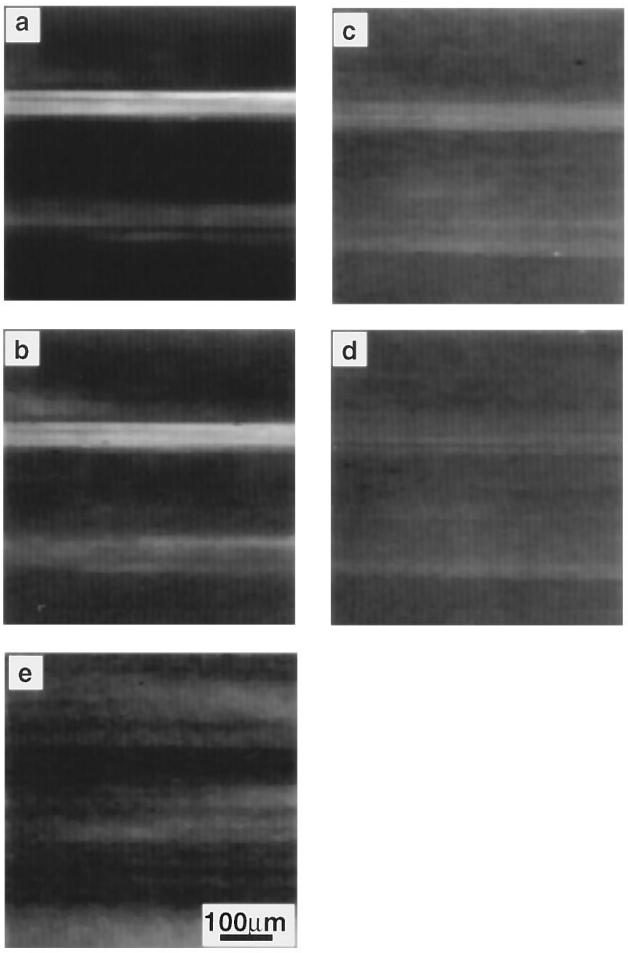

FIG. 4. CL filtered images of the (001) surface of the [110] compressed specimen: (a) D1, (b) D2, (c) D3, and (d) D4 images.

observations. In some cases, the specimen surfaces were etched with Sirtl or Wright solution to facilitate observation of the dislocation distributions by means of secondary electron imaging. Such etching did not affect the CL images. Transmission electron microscope (TEM) observation was also conducted to determine the types of dislocations.

Though the luminescence from an individual dislocation was too weak to be detected, CL from slip lines was intense enough to be observed. The dislocation configurations of the specimens are illustrated in Fig. 1.

Hydrogen plasma treatment was conducted for each specimen to check the effect of nonradiative centers introduced during deformation. Details of the condition of hydrogenation were described by Sekiguchi *et al.*[20] Most of the CL images described below were taken from the hydrogenated specimens if not otherwise mentioned.

Cathodoluminescence observation was performed with a quantitative pulse electron beam tester. A newly developed CL system was installed in a scanning electron microscope (TOPCON DS130) with a beam blanking system.[21] Specimens were excited by a pulsed electron beam with a chopping frequency of 333 Hz. The excitation energy and current were 20 kV and 1.5 nA, respectively. The light was collected with an ellipsoidal mirror and led by an optical fiber to a detection unit. A Jobin Yvon HR320 monochromator was used to record the CL spectrum. A set of band-pass filters was used for CL imaging. The characteristics of the filters are shown in the upper part of Fig. 2. Central energies of the filters coincide with the peak energies of D lines and the TO phonon replica of excitonic luminescence [abbreviated as EX(TO) hereafter]. An example of a photoluminescence spectrum in a weakly deformed specimen is shown in the lower part of Fig. 2. CL was detected by a Ge detector (North Coast EO-817L) with a lock-in amplifying technique. Such a modulated amplifying technique is indispensable in detecting the absolute value of luminescence. The time constant of the lock-in amplifier was set at 10 ms and the waiting time to record one pixel data was set at 12 ms. Signals were sent to the microcomputer and the absolute values of signals were recorded into an array of 160×160 pixel with 12-bit resolution. A median filter was applied to the image files to remove the shot noise of Ge detector.

III. RESULTS

A. CL from the specimen compressed along the [123] axis

Figure 3 shows a set of CL filtered images of the $(\overline{111})$ surface of a specimen compressed along the [123] axis (abbreviated as the [123] compressed specimen) together with a secondary electron image after etching. Slip lines are distin-

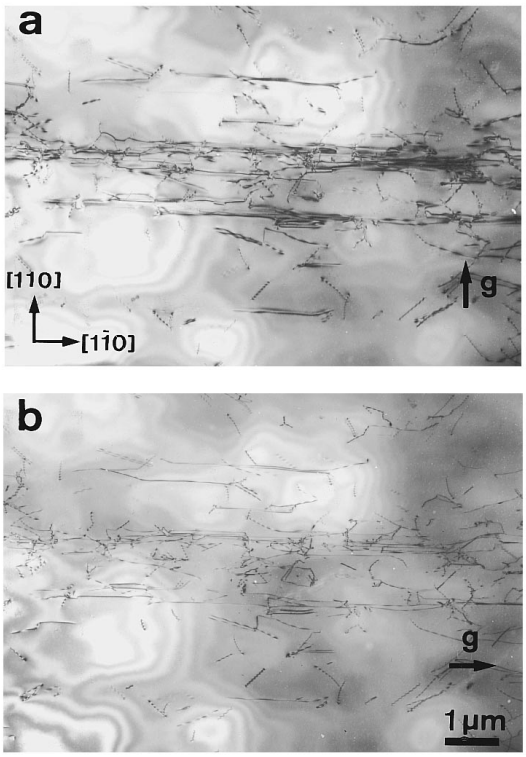

FIG. 5. TEM micrographs of dislocations on the (001) surface of the [110] compressed specimen: (a) $g=220$ and (b) $g=2\bar{2}0$.

guished by rows of etch pits in the secondary electron image. In this deformation, only dislocations of a single slip system are dominantly introduced and the reaction between dislocations belonging to different slip systems does not take place. Slip lines are seen as dark bands in the CL image taken using an EX(TO) filter [abbreviated as EX(TO) image]. Most slip lines are observed as bright bands in the D3 and D4 images, although some are not bright. On the other hand, it is difficult to detect slip lines in the D1 and D2 images.

B. CL from the [110] compressed specimen

Figure 4 shows the CL images of the (001) surface of a [110] compressed specimen. Bright bands along the [110] direction are clearly seen in D1 and D2 images while no significant luminescence is observed in D3 and D4 images. Observation of dislocation etch pits of the (1$\bar{1}$0) side surface showed that these regions of bright bands exactly coincide with the intersections of active (111) and (11$\bar{1}$) slip planes.

Figure 5 shows transmission electron microscopic (TEM) images of the region of the bright band in Fig. 4 taken under the two-beam condition. The diffraction vectors in Fig. 5(a) and 5(b) are $g=220$ and $g=2\bar{2}0$, respectively. We observe Lomer–Cottrell dislocations together with glide dislocations. The fraction of Lomer–Cottrell dislocations is less than 20%.

Figures 6 and 7 show the CL images of the different parts of the (1$\bar{1}$0) surface of a [110] compressed specimen. In the region of Fig. 6, one set of slip lines is introduced. Slip lines are seen as dark bands in the EX(TO) image, whereas they are observed as bright bands in the D3 and D4 images.

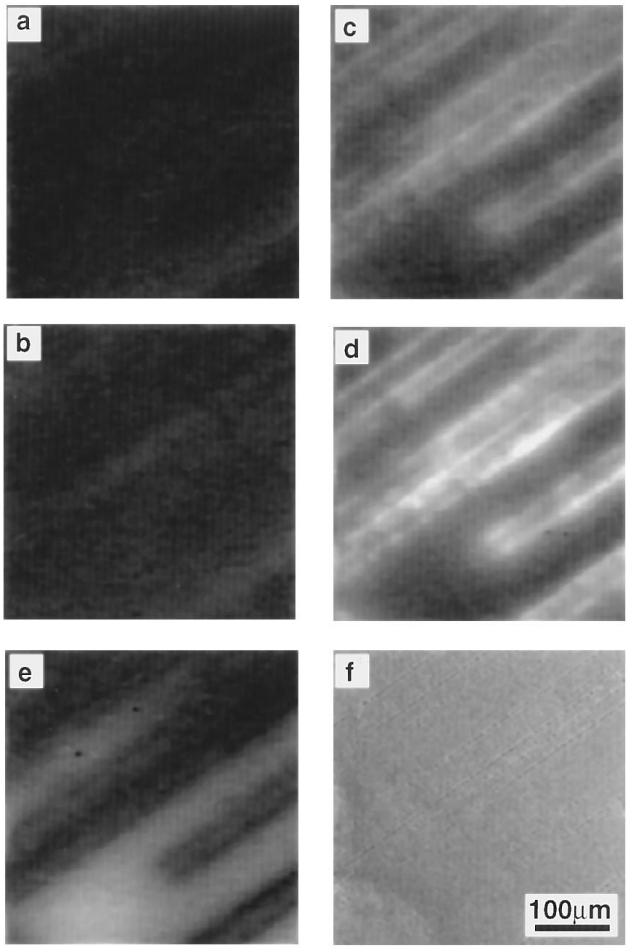

FIG. 6. CL filtered images of the (1$\bar{1}$0) surface of the [110] compressed specimen, where one set of slip lines is introduced: (a) D1, (b) D2, (c) D3, and (d) D4 images.

In the D1 and D2 images, on the other hand, it is difficult to detect slip lines. In Fig. 7, two sets of slip lines are introduced. D1 and D2 are very strong at the intersections of these lines, whereas D3 and D4 are observed along the slip lines. The maximum intensities of D1 and D2 at the intersections are stronger than those of D3 and D4.

Figure 8 shows the variation of CL spectra along a slip line in Fig. 7. The number assigned to each spectrum shows its location in Fig. 7(c). D1 and D2 are strong at point 1 (the intersection of slip lines), whereas D3 and D4 are strong at points 2 and 3 (non-intersecting points).

C. CL from the [120] or the [11 11 $\bar{6}$] compressed specimens

Figure 9 shows the CL images of the (001) surface of a [120] compressed specimen. The bright bands, which have been confirmed to be located at the intersections of active (111) and (11$\bar{1}$) slip planes by etch pits on the (210) side surface, are clearly seen in all the D line images. The intensity distributions along these bands in the D1 and D2 images are similar to each other, as are those of D3 and D4. Intensities of the D1 and D2 luminescence are not uniform along these bands, whereas those of D3 and D4 are rather uniform. The background in D3 and D4 images are rather high.

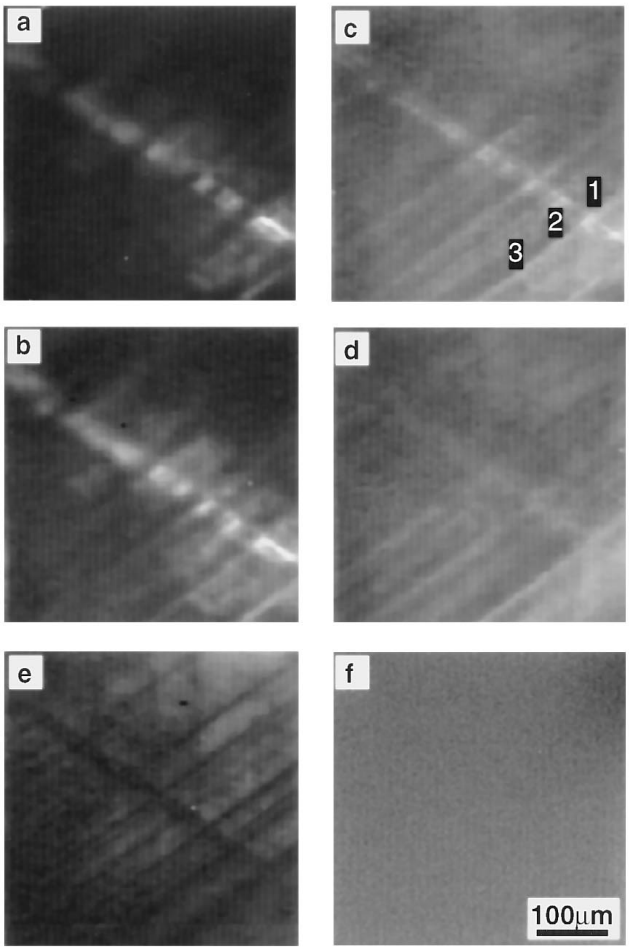

FIG. 7. CL filtered images of the $(1\bar{1}0)$ surface of the [110] compressed specimen, where two sets of slip lines intersect each other: (a) D1, (b) D2, (c) D3, and (d) D4 images.

Figure 10 shows CL images of the (3 3 11) surface of a [11 11 6] compressed specimen. A bundle of the slip lines is developed along the [110] direction on this surface, and correspondingly, the bright bands are observed in D3 and D4 images.

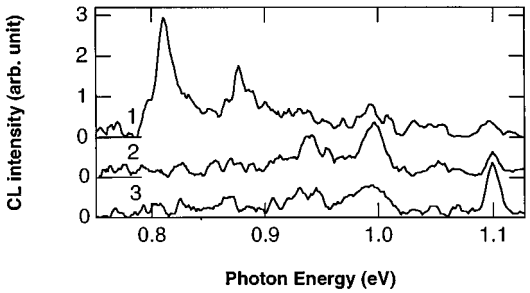

FIG. 8. CL spectra from different positions along a slip line in Fig. 7. The numerals indicate the positions in the image in Fig. 7(c). Position 1 is the intersection of slip lines. Positions 2 and 3 are the nonintersecting points.

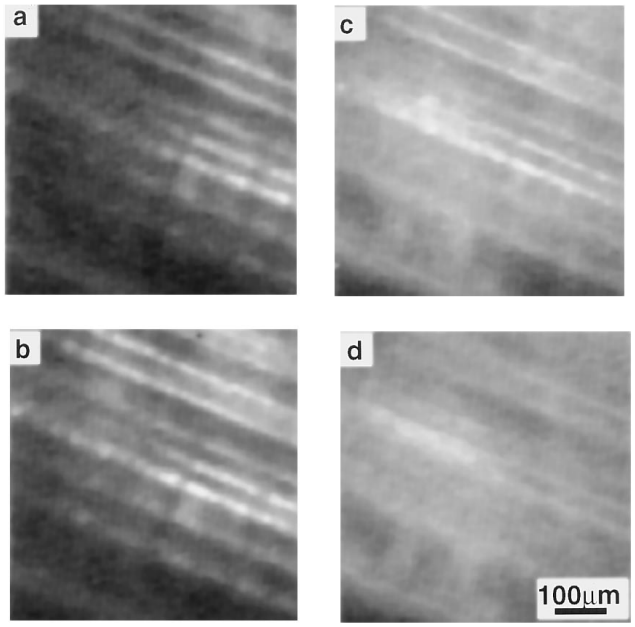

FIG. 9. CL images of the (001) surface of the [120] compressed specimen: (a) D1, (b) D2, (c) D3, and (d) D4 images.

D. Effect of hydrogen treatment

The effect of hydrogenation was tested for all the specimens. It was not remarkable in comparison with the case of the specimen deformed by scratching at room temperature.[20] One exception was the case of the (001) surface of the [120] compressed specimen. In this case, hydrogen treatment enhanced the CL images significantly. Figure 11 shows the CL images before hydrogen treatment. The correlation of the bright regions and dislocation slip lines are not clear due to the background especially in the D3 and D4 images. The

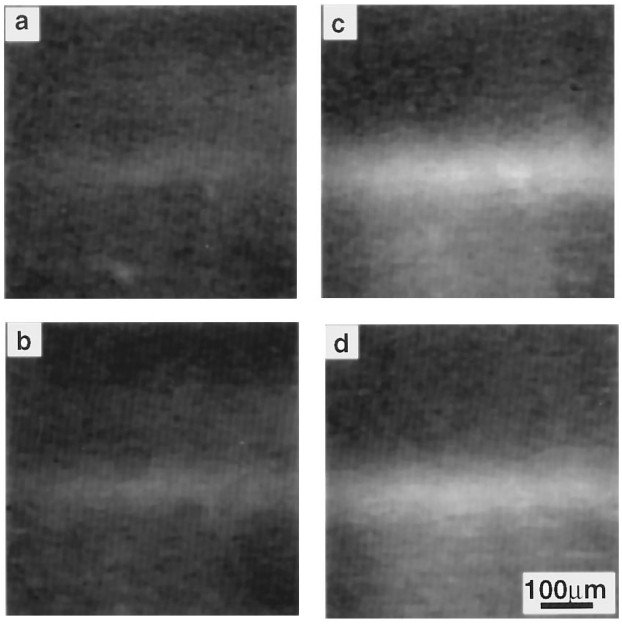

FIG. 10. CL images of the (3 3 11) surface of the $[11\ 11\ \bar{6}]$ compressed specimen: (a) D1, (b) D2, (c) D3, and (d) D4 images.

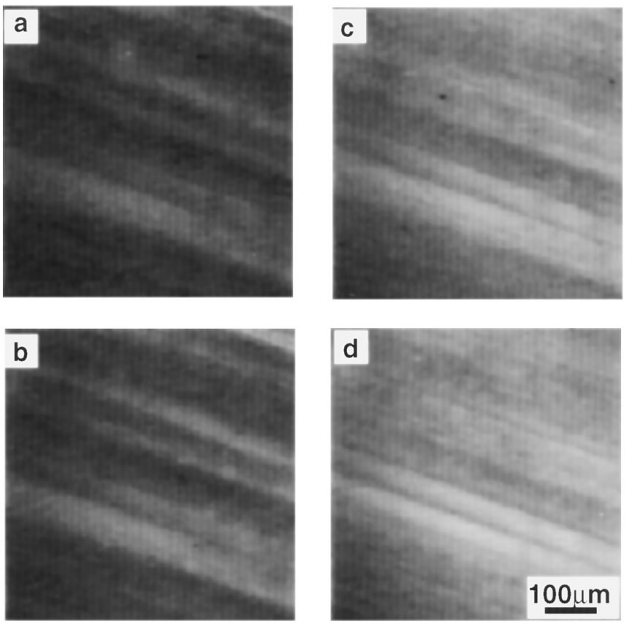

FIG. 11. CL filtered images of the (001) surface of the [120] compressed specimen before hydrogen treatment: (a) D1, (b) D2, (c) D3, and (d) D4 images.

luminescence from the intersections of slip planes become strong in all the D line images after hydrogen treatment (Fig. 9).

IV. DISCUSSION

A. Distribution of D line luminescence

The slip lines on the $(\overline{111})$ surface of the [123] compressed specimen (Fig. 3) and those on the (110) surface of the [110] compressed specimen (Fig. 6) are bright in D3 and D4 images, whereas they do not give rise to D1 and D2 luminescence. This shows that glide dislocations act as radiative centers of D3 and D4 luminescence. If we compare these two specimens, the slip lines in the latter specimen are more intense and sharper than those in the former specimen. Since two equivalent slip systems are activated in the latter specimen while only one system is activated in the former, the distributions of dislocations in these two specimens are thought to be different from each other, resulting in the above difference in these D line luminescences.

In contrast to the situation in these regions, the intersections of the two sets of slip lines in the [112] and [112] directions on the (110) surface of the [110] compressed specimen are bright in D1 and D2 images as shown in Fig. 7. The two sets of slip lines are visible as bright bands in the D3 and D4 images. This leads to the idea that D1 and D2 luminescence appears in the region where a reaction takes place between dislocations on the (111) slip plane and those on the (111) slip plane. The variation of the CL spectrum along a slip line (Fig. 8) supports such an idea.

In Fig. 4, on the (001) front surface of the [110] compressed specimen, the regions of intersections of the (111) and (111) slip planes were confirmed to be very bright in D1 and D2 images, while they are rather faint in D3 and D4 images. TEM observation shows that the fraction of Lomer–Cottrell dislocations is less than 20% in this region. This may suggest that Lomer–Cottrell dislocations act as the luminescence centers of D1 and D2.

As has been shown in Table I, the [110], [120], and [11 11 6] compressions give rise to dislocation reactions. On the (001) surface of the [110] compressed specimen, D1 and D2 are bright along the intersections of the (111) and (111) slip planes, while D3 and D4 are faint. To the contrary, the regions of intersections of slip planes are bright in all the D line images on the (001) surface of the [210] compressed specimen. The region of a slip line bundle on the (3 3 11) surface of the [11 11 6] compressed specimen is bright in the D3 and D4 images, whereas it is very faint in the D1 and D2 images. The possible products of the dislocation reaction in the [110] compressed specimen are Lomer–Cottrell dislocations and jogs and those in the [120] compressed specimen are only jogs, while no such reactions take place in the [11 11 6] compressed specimen. We may conclude that both Lomer–Cottrell dislocations and jogs act as the radiative centers for D1 and D2 luminescence.

On the (001) surface of the [110] compressed specimen, D3 and D4 are very weak compared with D1 and D2 in spite of the fact that glide dislocations also exist together with Lomer–Cottrell dislocations. The intensities of D1 and D2 luminescence are several times stronger than those of D3 and D4 luminescence on the (110) surface of the same specimen. The intensity of luminescence is written as

$$I_{Di} \propto N_{Di} \cdot \sigma_{Di} / \sum_j N_j \cdot \sigma_j , \tag{1}$$

where I_{Di} is the intensity of ith luminescence, and N_j and σ_j are the density and the capture cross section of the jth carrier recombination process, respectively. The summation should be done for all the carrier recombination processes, both radiative and nonradiative. If the Lomer–Cottrell dislocation is accompanied by high density of D1 and D2 centers or big capture cross sections for D1 and D2 luminescence, the strong D1 and D2 recombinations may mask the D3 and D4 recombinations. The fraction of Lomer–Cottrell dislocations is less than 20% of the total dislocations. Hence, the centers of D1 and D2 may be more densely distributed along Lomer–Cottrell dislocations than those of D3 and D4 along the glide dislocations. Alternatively, the centers of D1 and D2 luminescence at the Lomer–Cottrell dislocations may have much bigger capture cross section than those of D3 and D4 at glide dislocations.

The D1 and D2 images are always similar to each other in all kinds of specimens. The same holds for the D3 and D4 images. This may indicate that the centers for D1 and D2 luminescence are produced by the same dislocation process, and the same holds true for the centers of D3 and D4. The intensity ratio of D1 to D2 and that of D3 to D4 vary along slip lines. This suggests that D1 is not the phonon replica of D2 luminescence and that D3 is not that of D4, contrary to the report by Weronek *et al.*[17]

B. Origin of D1 and D2 luminescence

Shreter *et al.*[22] attributed the dislocation-related photoluminescence to the one-dimensional energy band caused by the deformation potential. In the first approximation, they insist that the energy of dislocation-related PL lines, $h\omega$, can be roughly given by

$$h\omega = E_g - A(b_e/a)^2, \tag{2}$$

where E_g is the gap width, a the lattice constant, A the coupling constant, and b_e the edge component of the Burgers vector. They attributed D1 luminescence to 90°-perfect interstitial prismatic loops or Lomer–Cottrell type dislocations and D2 to Frank partial dislocations, respectively.

Our study indicates that not only Lomer–Cottrell type dislocations but also jogs may yield D1 and D2 luminescence. Our specimens may include super-jogs formed by the intersection of dislocations. Since a super-jog has the same edge component as a Lomer–Cottrell dislocation, a super-jogs may also yield photons with energy similar to that of Lomer–Cottrell dislocations according to Shreter's hypothesis.[23] If we assume that the intensity of D line luminescence is proportional to the length of dislocation, a Lomer–Cottrell dislocation may give rise to stronger luminescence than that of super-jogs, because the length of a Lomer–Cottrell dislocation is much longer than that of super-jogs. This idea may explain our observations.

C. Effect of hydrogen

The effect of hydrogenation was much less remarkable in the specimens of the present work compared with the specimens scratched at room temperature.[20] This indicates that the density of nonradiative recombination centers in the former specimens is much smaller than that in the latter specimen. It is known that deformation induces both radiative and nonradiative recombination centers in a specimen and that most nonradiative recombination centers are related to point defects. Since the deformation took place at 800 °C in the present work, most of the nonradiative centers may have been annealed out after deformation. Only the [120] compressed specimens showed the hydrogen effect on the D lines as can be seen in Figs. 9 and 11. The regions of intersections of slip planes turned to be bright in all the D line images after hydrogen treatment. Since the most probable dislocation reaction in the [120] compression is jog formation, a higher density of nonradiative centers may be introduced than in the specimens deformed along other axes. Therefore, hydrogen passivation of nonradiative centers must be the most significant in this specimen.

Higgs *et al.*[18] state that D1 and D2 are strong in the regions between slip lines, while D3 and D4 are observed along slip lines. If we deform a crystal heavily, the dislocation reaction is enhanced and is thought to yield a high density of point defects acting as nonradiative centers. It is natural to assume that such nonradiative centers may modify D line images and that D line luminescence no longer reflects the dislocation distribution pattern. In such a case, hydrogen treatment might alter the D line images. The discrepancy between our results and those of Higgs might be interpreted in terms of this idea.

D. Effect of metal contamination

Higgs and Lightowlers reported that the D line luminescence is correlated with the metallic impurities.[24,25] They introduced dislocations into a silicon crystal under contamination-free conditions, and then contaminated the specimens with Cu, Ni, and Fe at different levels of contamination. They investigated the luminescence in such specimens and found that only low-level contamination of such impurities enhances D1 and D2 luminescence significantly in the same way. They concluded that metallic impurities in the strain field of dislocation were the cause of D1 and D2 luminescence.

In this study, all of the specimens were treated in the same way so that the levels of contamination can be considered to be the same in all the specimens. However, D1 and D2 luminescence as well as D3 and D4 luminescence was observed depending on the dislocation configuration. Therefore it is difficult to attribute only D1 and D2 luminescence to the metallic impurities incorporated at the dislocation core.

V. CONCLUSION

(1) D1 and D2 luminescence is observed dominantly in the regions of the intersections of slip lines, whereas D3 and D4 luminescence is detected along slip lines. D1 and D2 originate from the defects produced by the same dislocation processes; the same holds for D3 and D4. The former and the latter defects are different from each other in nature.

(2) D3 and D4 arise due to the glide dislocations. D1 and D2 originate from the reaction products of dislocations, namely Lomer–Cottrell dislocations and jogs.

(3) Hydrogen treatment enhances the D line images when a high density of point defects is introduced by plastic deformation.

(4) Metallic impurities do not seem to be related to D1 and D2 luminescence.

[1] F. D. Wohler, H. Alexander, and W. Sander, J. Phys. Chem. Solids **31**, 1381 (1970).
[2] V. V. Kveder, Yu. A. Ossipyan, W. Schroter, and G. Zoth, Phys. Status Solidi A **72**, 701 (1982).
[3] H. Ono and K. Sumino, J. Appl. Phys. **57**, 287 (1985).
[4] J. R. Chelikowski, Phys. Rev. Lett. **49**, 1569 (1982).
[5] K. W. Lodge, A. Lapiccirella, C. Battistoni, N. Tomassini, and S. L. Altmann, Philos. Mag. A **60**, 643 (1989).
[6] S. Winter, Phys. Status Solidi B **90**, 289 (1978).
[7] H. Teichler, J. de Phys. **40**, C6-43 (1979).
[8] N. A. Drozdov, A. A. Patrin, and V. D. Tkachev, Pis'ma Zh. Eksp. Teor. Fiz. **23**, 651 (1976) [JETP Lett. **23**, 597 (1976)].
[9] N. A. Drozdov, A. A. Patrin, and V. D. Tkachev, Phys. Status Solidi B **83**, K137 (1977).
[10] M. Suezawa, Y. Sasaki, and K. Sumino, Phys. Status Solidi A **79**, 173 (1983).
[11] R. Sauer, J. Weber, J. Stolz, E. R. Weber, K.-H. Kusters, and H. Alexander, Appl. Phys. A **36**, 1 (1985).
[12] Yu. Lerikov, Yu. Rebane, S. Ruvimov, D. Tarhin, A. Sitnikova, and Yu. Shreter, *Proceeding of the 16th International Conference on Defects in Semiconductors*, edited by G. Davies, G. G. DeLeo, and M. Stavola (Trans

Tech, Zurich, 1992) [Mater. Sci. Forum **83–87**, 1321 (1992)].
[13] M. Suezawa and K. Sumino, Phys. Status Solidi A **78**, 639 (1983).
[14] M. Suezawa, K. Sumino, and Y. Nishina, Jpn. J. Appl. Phys. **21**, L518 (1982).
[15] R. Sauer, Ch. Kisielowski-Kemmerich, and H. Alexander, Phys. Rev. Lett. **57**, 1472 (1985).
[16] M. Suezawa, Y. Sasaki, Y. Nishina, and K. Sumino, Jpn. J. Appl. Phys. **20**, L537 (1981).
[17] K. Weronek, J. Weber, A. Hopner, F. Ernst, R. Buchner, M. Stefaniak, and H. Alexander, *Proceedings of the 16th International Conference on Defects in Semiconductors*, edited by G. Davies, G. G. DeLeo, and M. Stavola (Trans Tech, Zurich, 1992) [Mater. Sci. Forum **83–87**, 1315 (1992)].
[18] V. Higgs, E. C. Lightowlers, C. E. Norman, and P. C. Kightley, *Proceedings of the 16th International Conference on Defects in Semiconductors*, edited by G. Davies, G. G. DeLeo, and M. Stavola (Trans Tech, Zurich, 1992) [Mater. Sci. Forum **83–87**, 1309 (1992)].
[19] W. Kane, RCA Rev. **31**, 187 (1970).
[20] T. Sekiguchi, V. V. Kveder, and K. Sumino, J. Appl. Phys. **76**, 7882 (1994).
[21] T. Sekiguchi and K. Sumino, Rev. Sci. Instrum. **66**, 4277 (1995).
[22] Yu. G. Shreter, Yu. T. Rebane, and A. R. Peaker, Phys. Status Solidi A **138**, 681 (1993).
[23] Y. Shreter and T. Sekiguchi (private communication).
[24] V. Higgs, C. E. Norman, E. C. Lightowlers, and P. C. Kightley, *Proceedings of the 20th International Conference on the Physics of Semiconductors*, edited by E. M. Anastassakis and J. D. Joannopoulos (World Scientific, Singapore, 1990), Vol. 1, p. 706.
[25] V. Higgs, E. C. Lightowlers, and P. C. Kightley, *Materials Research Society Symposia Proceedings*, Vol. 163, edited by D. J. Wolford, J. Bernholc, and E. Haller (MRS, Pittsburg, PA, 1990), p. 57.